Diastereoselective Indole-Dearomative Cope Rearrangements by Compounding Minor Driving Forces.
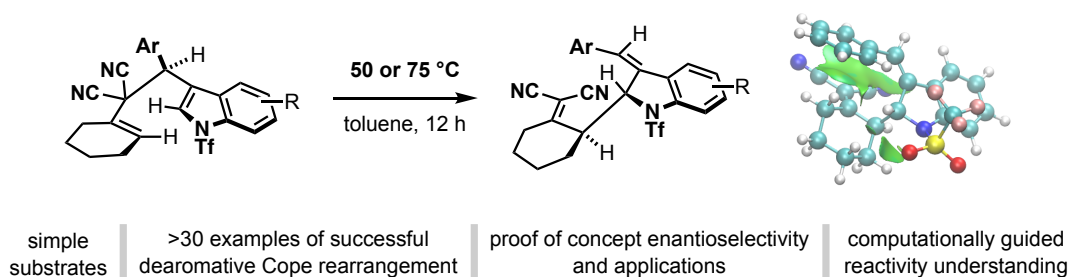
Dr. Subhadip De, Breanna Tomiczek, Yinuo Yang, Kenneth Ko, Dr. Ion Ghiviriga, Prof. Adrian Roitberg*,

Prof. Alexander J. Grenning *

Department of Chemistry, University of Florida

PO Box 117200 Gainesville, FL 32611

grenning@ufl.edu; roitberg@ufl.edu

| simple substrates | >30 examples of successful dearomative Cope rearrangement | proof of concept enantioselectivity and applications | computationally guided reactivity understanding |

Abstract

Reported herein is the discovery of a diastereoselective indole-dearomative Cope rearrangement. A suite of minor driving forces (substrate destabilizing effects; product stabilizing effects) are what promote this otherwise unfavorable dearomatization reaction. These include the following that work *in concert* to overcome the penalty for dearomatization: (i.) steric congestion in the starting material, (ii.) alkylidene malononitrile and stilbene conjugation events in the product, and (iii.) an unexpected intramolecular π–π* stack on the *product side* of the equilibrium. The key substrates are rapidly assembled from alkylidenemalononitriles and indole-phenylmethanol derivatives resulting in many successful examples (high yields and diastereoselectivity). The products are structurally complex bearing vicinal stereocenters generated by the dearomative Cope rearrangement. They also contain a variety of functional groups for interconversion to complex architectures. On this line, also described herein are proof-of-concept strategies for achieving enantioselectivity and conversion of the dearomative products to valuable and functionalized small drug-like molecules.

Introduction

Aromatic sigmatropic rearrangements involving dearomatized intermediates and/or products often leverage a heteroatom to facilitate and favor dearomatization and/or aromatic functionalization. This is because of the generally favorable kinetics and thermodynamics of such systems. As such, there is a rich variety of "heteroatomic 1,5-diene" substrates classes reported in (Figure 1A),[1-20] including many "named reactions" (aromatic Claisen-[21] and Sommelet-Hauser-[22] rearrangements; Fischer indole synthesis[23]). The all-carbon analogs (1,5-dienes; Cope rearrangement substrates[24]) are more challenging, energetically speaking.[25] They are innately unfavorable rearrangements thermodynamically ($\Delta G = 0$). This degeneracy can be broken in productive ways (e.g. the oxy-Cope rearrangement[26]) or unproductive ways (e.g. the aromatic Cope rearrangement) (Figure 1B). Regarding the later, aromatic Cope rearrangements are relatively rare with few modern examples applicable to complex molecule synthesis.[27] The most common strategy to drive forward an aromatic Cope rearrangement is to utilize strain release (Figure 1C, eq 1).[28-30] There are also some historical reports related to anion-acceleration (Figure 1C, eq 2).[31] A relatively new strategy put forth

Figure 1. *Aromatic sigmatropic rearrangements.* **A:** *There is a rich diversity of heteroatomic substrate classes.* **B:** *Modern strategies for promoting aromatic Cope rearrangements leverage strain-release and "synchronized" aromaticity.* **C:** *Heteroatomic 1,5-dienes (and aromatic counterparts) are innately reactive whereas all-carbon 1,5-dienes are not. This challenge is exacerbated in the case of aromatic Cope substrates.*
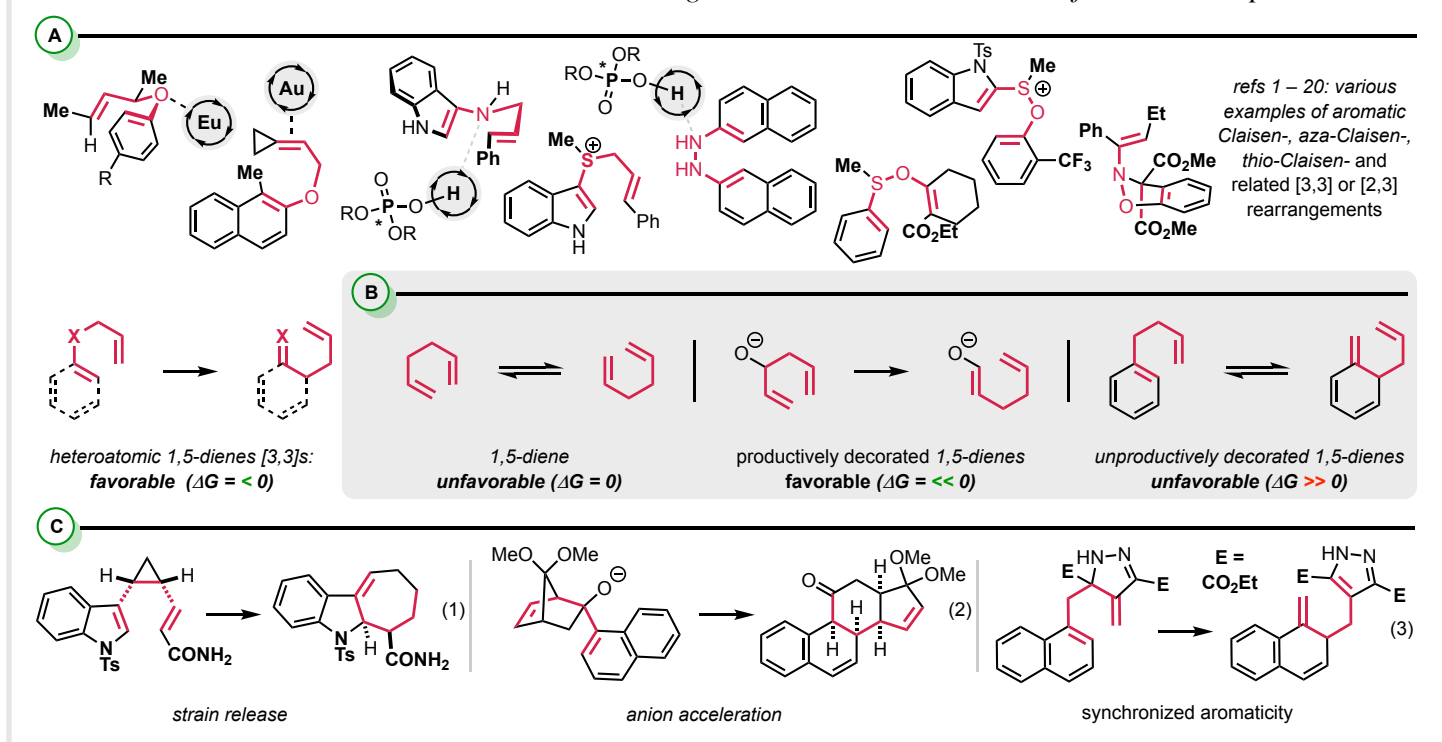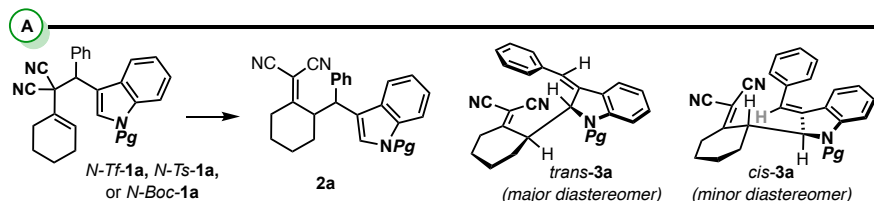
by Frantz and coworkers pertains to *synchronized* aromaticity (Figure 1C, eq 3).[32] Considering the relative dearth of methods for achieving aromatic Cope rearrangement, there is a need to identify new methods of value to complex molecule synthesis. Qualities of these methods should include (a) desirable energetic profiles (low kinetic barrier; high thermodynamic favorability) and (b) stereocontrol about the [3,3] rearrangement yielding (c) valuable small molecules (pharmaceutical leads, natural products) from (d) readily available starting materials. Our previous work resulted in the discovery of 3,3-dicyano-1,5-dienes (and related substrates) that have low [3,3] kinetic barriers (19 – 25 kcal/mol), high thermodynamic favorability ($\Delta G = -5$ kcal/mol), and yield useful building blocks containing vicinal stereocenters.[33,34] These findings suggest that other more challenging Cope substrate classes may be positively impacted by related engineering strategies. Herein, we report the discovery of a readily available class of substrate capable of undergoing thermodynamically favorable indole-dearomative Cope rearrangement.
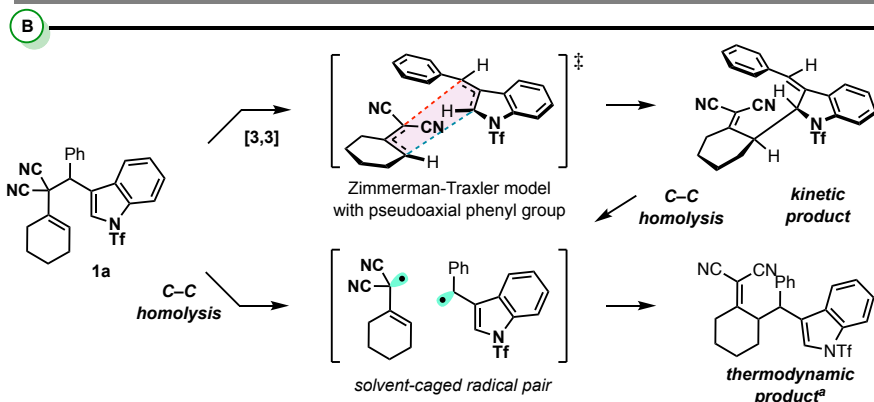
RESULTS & DISCUSSION

Vicinal stereocenter-generating, dearomative Cope rearrangement was first observed on substrate **1a** (Figure 2A), though we examined other related model systems with limited success thus far (see supporting information). This substrate has some rationally designed features which we hypothesized would favor the desired dearomative Cope rearrangement. For example, in addition to facilitating substrate synthesis, the 3,3-dicyano moiety would stabilize the transition state and the product-side of the equilibrium through resonance conjugation. For similar reasons, the 4-phenyl group would facilitate and partially counteract the penalty for indole-dearomatization. And together, the 3,3-dicyano and the 4-phenyl group weaken the C3–C4 bond *via* torsional strain/steric congestion. Thus, there is both substrate-destabilizing features and product-stabilizing features designed into the starting material. It was found that at elevated temperatures the [1,3] Cope product **2a** was favored (Figure 2A, entry 1), likely *via* a solvent-caged radical route (Figure 2B and 2D). However, temperatures ranging from rt – 100 °C produced the desired [3,3] product *trans*-**3a** with two new vicinal stereocenters and *trans*-stilbene geometry exclusively (Figure 2A, entries 2 – 6). This stereochemistry was
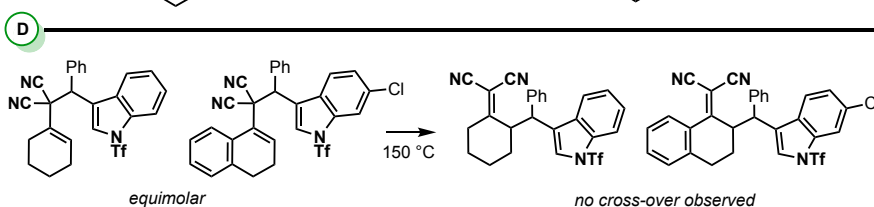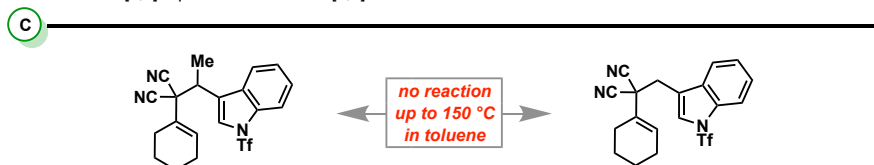
Figure 2. A: *[1,3] vs [3,3] Cope rearrangements.* **B:** *Mechanistic considerations for the competing pathways.* **C:** *Probing the impact of the 4-phenyl group on rearrangement reactivity.* **D:** *A cross-over experiment pertaining to the radical [1,3] rearrangement.*

A

N-Tf-**1a**, N-Ts-**1a**, or N-Boc-**1a**

2a

*trans-***3a** (major diastereomer)

*cis-***3a** (minor diastereomer)

entry	temp (°C)	solvent	time (hrs)	Pg	conv. (%)	2a : 3a	% yield 3a	trans- 3a : cis- 3a	% yield 2a	dr of 2a
1	150	tol	15	Tf	100	1:0	–	–	74% yield	1:1
2	100	tol	15	Tf	100	1:1	46% yield	4:1	45% yield	3:1
3	75	tol	15	Tf	100	0:1	88% yield	>20:1	–	–
4	75	tol	8	Tf	78	0:1	–	>20:1	–	–
5	50	tol	15	Tf	50	0:1	48% yield	>20:1	–	–
6	rt	tol	7 d	Tf	25	0:1	–	>20:1	–	–
7	75	DMA	15	Tf	77	0:1	–	7.5:1	–	–
8	75	THF	15	Tf	70	0:1	–	9:1	–	–
9	75	ACN	15	Tf	81	0:1	–	10:1	–	–
10	75	DMF	15	Tf	65	0:1	–	16:1	–	–
11	50	DCM	15	Tf	33	0:1	–	>20:1	–	–
12	75	tol	15	Ts	46	0:1	–	5:1	–	–
13	75	tol	15	Boc	0	0:0	–	–	–	–
14	100	tol	15	Boc	81	1:0	–	–	–	1.7:1

B

1a

[3,3]

Zimmerman-Traxler model with pseudoaxial phenyl group

C–C homolysis

kinetic product

C–C homolysis

solvent-caged radical pair

thermodynamic product[a]

[a] both sides of [3,3] equilibrium convert to [1,3] at 150 °C

C

no reaction up to 150 °C in toluene

D

equimolar

150 °C

no cross-over observed

assigned based on detailed NMR analysis.[35] Notably, the transformation proceeded with high diastereoselectivity at 75 °C (Figure 2A, entry 3), but was less selective at 100 °C (Figure 2A, entry 2). The stereochemistry observed is rationalized by a closed, chair-like transition state, though the outcome also suggests that the 4-phenyl group is positioned pseudo-axial in this model (Figure 2B, top pathway). The optimal temperature is 75 °C as the transformation proceeded selectively in a reasonable time frame (15h, 100% conv., Figure 2A, entry 3). It was rather intriguing that the transformation also proceeds at rt and 50 °C, as this suggests that the transformation has a relatively low kinetic barrier. In other solvents, the reaction also progressed, often resulting in a second diastereomer,

which was characterized as the *cis*-stilbene analog *cis*-**3a** (Figure 2A, entries 7 – 11).[35] This diastereomer presumably arises from a chair-like transition state where the phenyl group is positioned pseudo-equatorial.

During the optimization studies, we also examined the effect of the *N*-protecting group and found that the *N*-Ts analog was less reactive under the optimized conditions and yielded a 3:1 diastereomeric mixture of Cope products (Figure 2A, entry 12). Similarly, *N*-Boc-**1a** was unreactive to [3,3] under the standard conditions (Figure 2A, entry 13) and at elevated temperature, only the formal [1,3] product was observed (Figure 2A, entry 14). As a final note related to optimization, it was also observed that the Cope product **3a** can directly convert to **2a**, either by a direct homolysis mechanism or a retro-[3,3] followed by C–C cleavage pathway (Figure 2B). To probe the significance of the 4-phenyl group on Cope rearrangement reactivity, we prepared substrates which bear a 4-methyl group and an unsubstituted methylene, respectively (Figure 2C). Neither of these substrates were reactive up to 150 °C providing qualitative support that the 4-phenyl group has a unique impact on the kinetics and thermodynamics of this dearomative transformation.

The thermodynamic favorability of this indole-dearomatizing Cope rearrangement and the observed *trans*-stilbene diastereoselectivity is intriguing. To support our substrate design hypotheses and initial observations, we turned to DFT computation (Figure 3). Recall, the observed diastereomers *trans*-**3a** and *cis*-**3a** are *trans*- and *cis*-stilbene isomers and are thus derived from chair transition states differing by either pseudo-axial or pseudo- equatorial positioning of the phenyl group, respectively (Figure 3A, equations 1 – 2). The computational data supports that the chair-pseudo-axial-phenyl transition state leading to the major observed *trans*-stilbene product *trans*-**3a** (Figure 3A, equation 1) is kinetically favored over the chair-pseudo-equatorial-phenyl transition state toward the minor observed diastereomer *cis*-**3a** (Figure 3A, equation 2); $\Delta\Delta G^{\ddagger}$ = 1.8 kcal/mol (Figure 3A, equation 1 *vs.* equation 2). Based on a Non-Covalent Interaction (NCI) analysis,[36,37] both pathways (equation 1 and 2) are exergonic. The key distinguishing feature in favor of equation 1 is an aromatic π–π^{*} interaction (secondary orbital overlap) between the developing alkylidenemalononitrile and *trans*-stilbene functional groups.[38] This interaction is significantly weaker in the pathway where the phenyl group is positioned pseudo-equatorial (equation 2), especially in the product (see SI for complete NCI analysis). For continuity, we also modeled the Cope rearrangements that proceed through boat transition states where the phenyl group is positioned either pseudo-axial (Figure 3A, equation 3) or

pseudo-equatorial (Figure 3A, equation 4)), and thus having the *trans*-stilbene or *cis*-stilbene geometry, respectively, in the product (Figure 3A, equations 3 – 4). In both cases, the reactive conformer and the transition state were found to be higher in energy than the comparative transformations that proceed *via* chair conformations, which agrees with the experimental findings. Interestingly, the product derived from the boat conformation with the phenyl group positioned pseudo-axial is quite thermodynamically favorable (ΔG = –3.3 kcal/mol), though not observed due to unfavorable kinetics compared to other pathways. Like the major
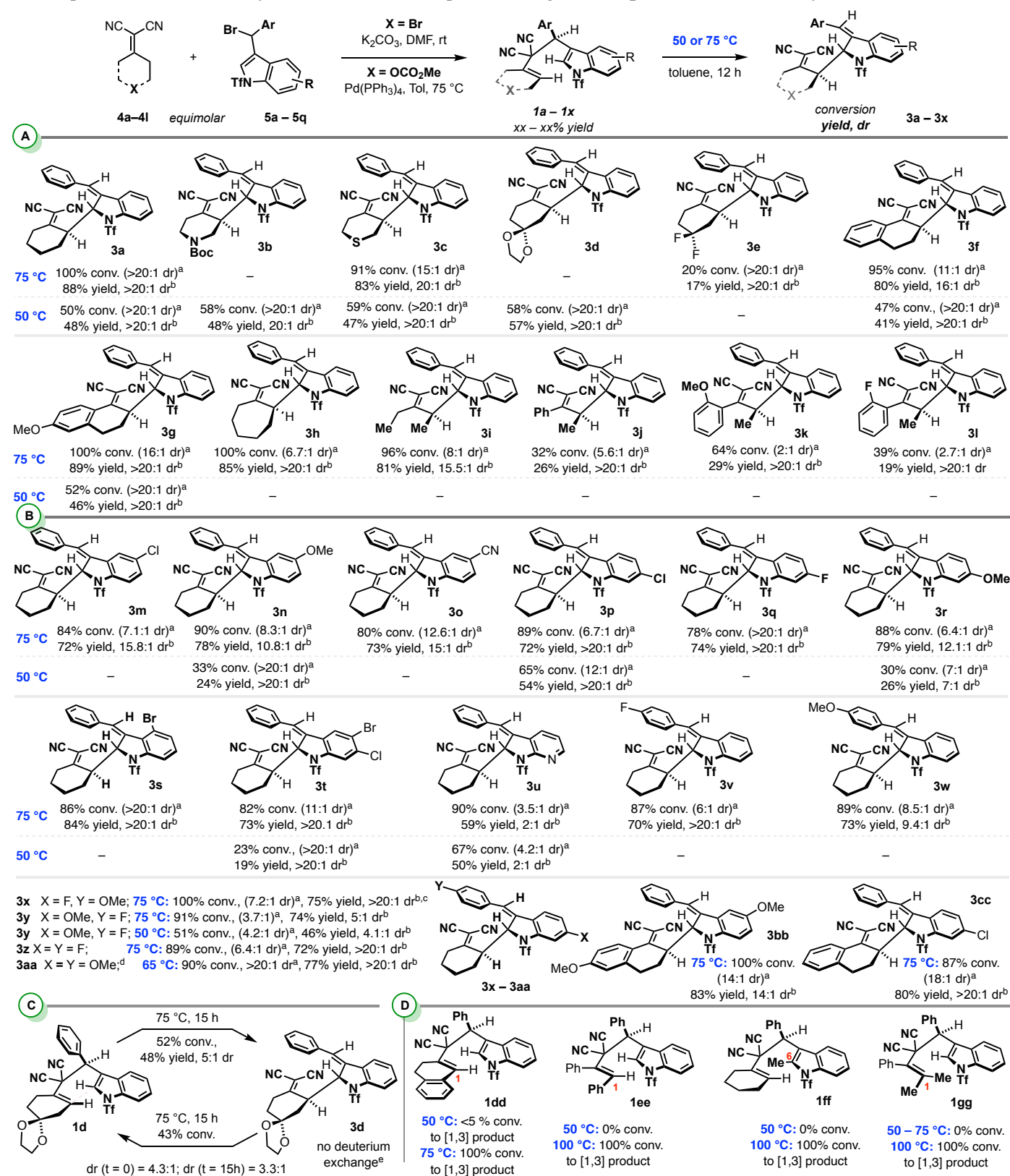

Figure 3. A: *Computational investigation of kinetics and thermodynamics of dearomative [3,3].* **B:** *Visualization of the potential dearomatized diastereomers with plotted NCI regions, indicating the key π-π* interaction that distinguishes the top pathway from the others.* **C.** *Computational investigation of the competing formal [1,3] rearrangement.*
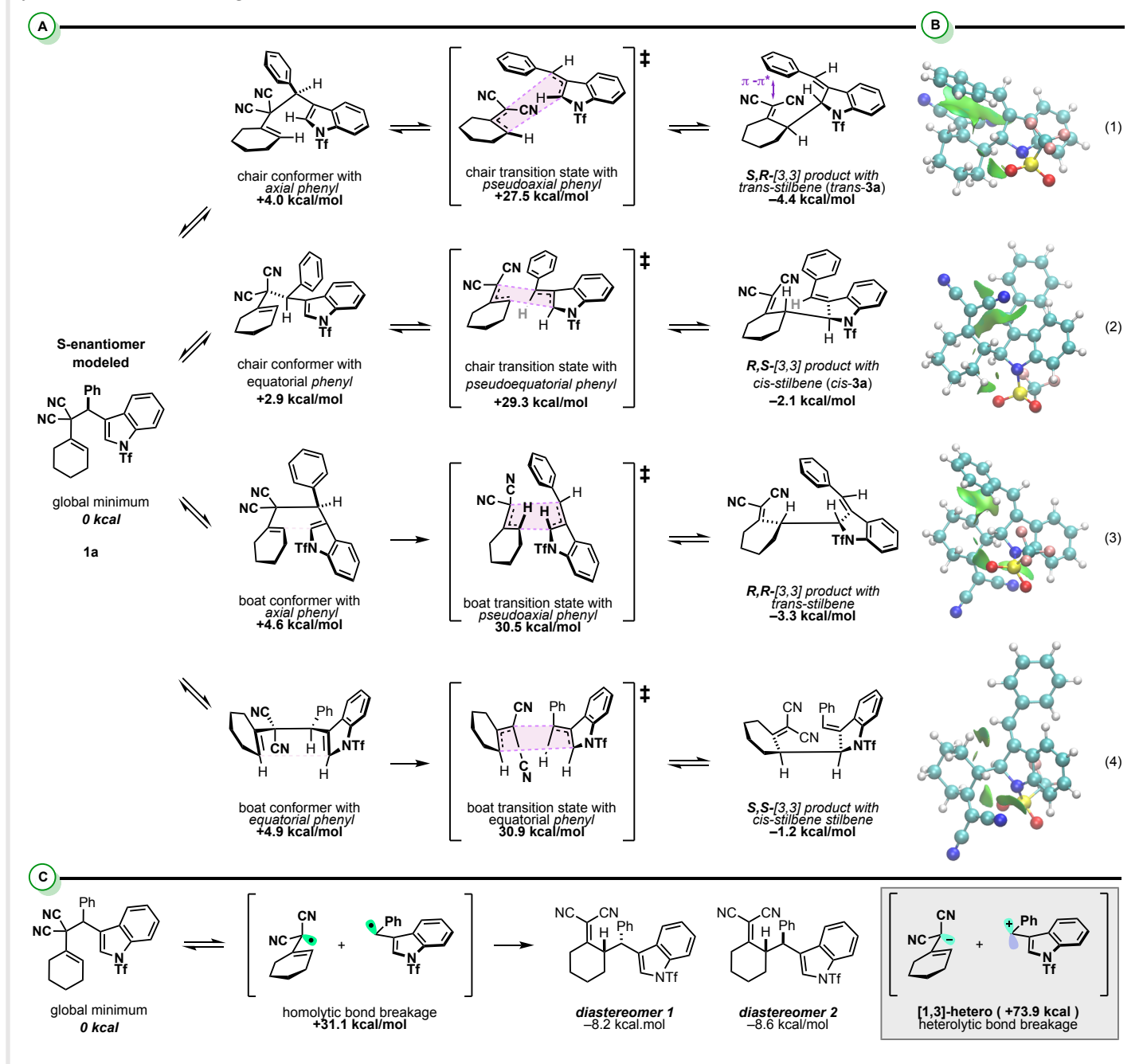
observed product *trans*-**3a**, the ground state has significant noncovalent stabilizing features, in this case C-H–π interaction between the cyclohexyl and styrene portions of the molecule. The calculations also support that the most kinetically- and thermodynamically- favorable dearomative Cope rearrangement pathway (Figure 3A, equation 1) is *kinetically favored* over the radical [1,3] rearrangement ($\Delta\Delta G^{\ddagger}$ = 3.6 kcal/mol) (Figure 3C). On this line, we also probed the likelihood of a radical *vs.* ionic [1,3] rearrangement. The calculations overwhelmingly favor the radical pathway. Gratifyingly, these computational observations are in line with the experimental findings. It is thought-provoking to realize that the favorability for dearomatization is achieved through the combination of many minor contributing structural features: C3–C4 congestion in the starting material, alkylidenemalononitrile and stilbene conjugation events in the product, and an aromatic π-π^{*} interaction.

With a method in hand for achieving indole-dearomatizing Cope rearrangement, we turned to examine the scope of the transformation (Figure 4). Standard conditions involved heating the substrate **1aa** – **1gg** in toluene at 75 °C. However, if diastereomers were observed, we often performed the reaction at 50 °C, which normally improved diastereoselectivity. As shown in Figure 4, we examined a variety of alkylidenemalononitriles **4** and indole-phenylmethanol-derived electrophiles **5** (bromides or carbonates). Figure 4A summarizes the scope with respect to various alkylidenemalononitriles. While the model cyclohexyl scaffold **3a** reached full conversion within 15 h, it was found that various cyclic scaffolds bearing functional groups at the 4-position often influenced the thermodynamics such that equilibrium mixtures of Cope "starting materials" **1** and Cope "products" **3** were observed (Figure 4D). Nonetheless, respectable yields of protected piperidine (**3b**; 52% yield), tetrahydrothiopyran (**3c**; 83% yield), and ketal-protected cyclohexanone (**3d**; 57% yield) could be isolated at 75 °C. In these cases, the Cope equilibrium isomers were separable, allowing for recycling of the starting material. However, the difluorocyclohexanone-containing product **3e** was poorly favored, thermodynamically. Next, it was found that tetralone- (**3f** – **3g**) and cycloheptanone- (**3h**) based scaffolds were highly reactive toward indole-dearomatizing Cope rearrangement. This can be rationalized by strain release (endocyclic cycloheptene → exocyclic cycloheptene) and increased conjugation, respectively,

Figure 4. *Scope Studies.* **A:** *Variable alkylidenemalononitriles.* **B:** *Variable indole-phenylmethanol-derived electrophiles.* **C:** *Unsuccessful substrates.* **D:** *Cope rearrangement equilibrium observed for certain substrates.*

3x X = F, Y = OMe; **75 °C:** 100% conv., (7.2:1 dr)[a], 75% yield, >20:1 dr[b,c]
3y X = OMe, Y = F; **75 °C:** 91% conv., (3.7:1 dr)[a], 74% yield, 5:1 dr[b]
3y X = OMe, Y = F; **50 °C:** 51% conv., (4.2:1 dr)[a], 46% yield, 4.1:1 dr[b]
3z X = Y = F;   **75 °C:** 89% conv., (6.4:1 dr)[a], 72% yield, >20:1 dr[b]
3aa X = Y = OMe;[d]   **65 °C:** 90% conv., >20:1 dr[a], 77% yield, >20:1 dr[b]

3bb **75 °C:** 100% conv. (14:1 dr)[a] 83% yield, 14:1 dr[b]

3cc **75 °C:** 87% conv. (18:1 dr)[a] 80% yield, >20:1 dr[b]

[a] Diastereomeric ratio of crude reaction mixture [b] Diastereomeric ratio after chromatography; dr improvement is a result of chromatographic separation. [c] X-Ray crystallographic structure obtained [d] The [3,3] rearrangement was observed upon Pd-catalyzed coupling of **4** and **5**. [e] Cope rearrangement equilibrium studies performed in 10:1 tol-d$_8$:CD$_3$OD: no deuterium incorporation observed on the substrate.

upon dearomative [3,3]. The final set of substrates are derived from acyclic alkylidenemalononitriles: dialkyl

product **3i** was observed with high thermodynamic favorability (81% yield, 15.5:1 dr). Aryl-alkyl containing

motifs were also examined; The phenyl-containing substrate had surprisingly poor conversion (**3j**, 32% conv.; 26% yield, >20:1 dr) under the standard conditions. We also examined *ortho*-substitution within this substrate class and found that electron-donating methoxy-group incorporation improved the conversion (to **3k**), and an electron-withdrawing fluorine atom resulted in similar conversion to the simple benzene ring (**3l**). Figure 4B summarizes the scope with respect to the various indole-phenylmethanol-derived electrophiles. Electron withdrawing- and donating- groups were generally tolerated about the indole-portion of the scaffold (**3m** – **3u**). The 7-azaindole scaffold had acceptable thermodynamic favorability for dearomative Cope rearrangement to **3u**, though the diastereoselectivity was low (3.5 – 4.2 : 1) in comparison to most other examples in Figure 4. The phenyl portion of the scaffold was similarly tolerant to electronic changes. For example, both 4-fluorophenyl (**3v**) and 4-methoxyphenyl (**3w**) reached >85% conversion with good, isolated yield and diastereoselectivity. Finally, examples **3x**– **3aa** contain either electronically "paired" (e.g., F-/MeO- or MeO-/F-) or "dissonant" (e.g., F-/F- or MeO-/MeO-) arene–indole rings. It was found that in all cases that conversion and isolated yields were high and diastereoselectivity ranged from excellent to modest. An X-ray structure of **3x** was also obtained, further validating the outcomes in this work. The final examples in Figure 4B utilized tetralone-based scaffolds (**3bb** / **3cc**). Figure 4C shows that within the indole-series, there are substrates that show no sign of dearomative Cope product rearrangement. The β-tetralone- and deoxy-benzoin-derived scaffolds **1dd** and **1ee** had little to no conversion at 50 °C. Further, 100% conversion to the [1,3] product was observed for these substrates at 75° and 100 °C, respectively. This can be rationalized by considering that the additional phenyl groups at the "1-position" will stabilize radical intermediates. We also found that the construction of quaternary carbons *via* dearomative [3,3] was not possible under the conditions examined (**1ff** – **1gg**). Figure 4D explored the possibility of hydrogen–deuterium exchange at the potentially acidic γ-position on **3** (Figure 4D). No deuterium was incorporated, suggesting that this position is not particularly acidic, unlike the unsubstituted alkylidenemalononitriles **1**.

We also examined substrates that present various regio- and stereochemical considerations (Figure 5). For example, we were interested in the azepane alkylidenemalononitrile **4p** due to the significance of

**Figure 5:** *Other regio- and/or stereochemical considerations related to the indole-dearomative Cope rearrangement.*
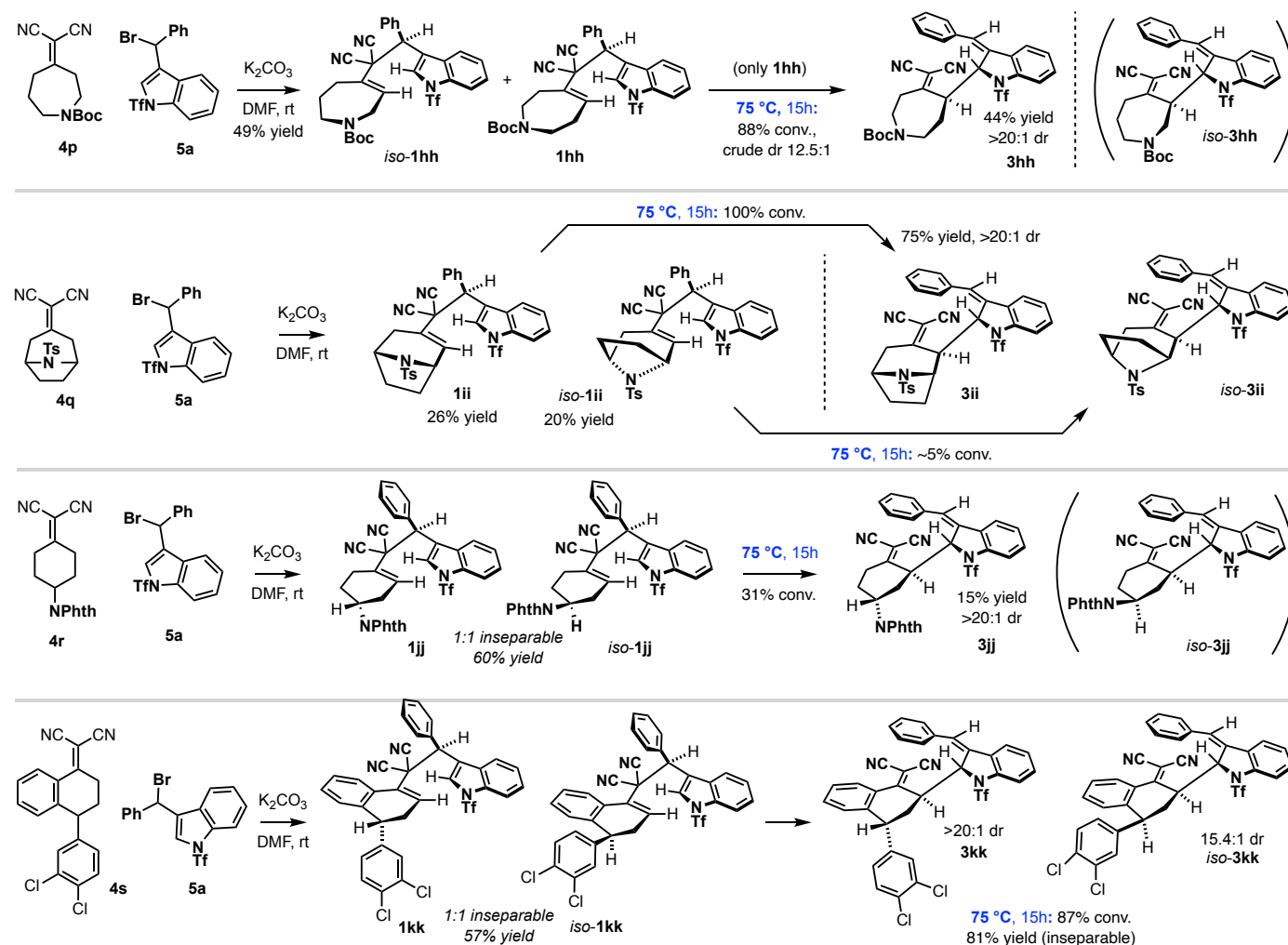
azepanes in drug discovery programs.[39] It was found that under the standard coupling conditions, that two regiomeric products **1hh** and *iso*-**1hh** were isolated (1.4:1 rr). This is attributed to the fact that there are only subtle differences in the pKa of the two non-equivalent γC–H groups on either side of the alkylidenemalononitrile. The regioisomers were isolated primarily as a mixture, though a small amount of **1hh** could be separated. This pure sample was subject to standard dearomative Cope rearrangement conditions yielding **3hh** in 44% isolated yield (>20:1 dr). The tropinone-derived alkylidenemalononitrile **4q** is prochiral. Two separable diastereomers **1ii** and *iso*-**1ii** were observed upon coupling between **4q** and **5a**. These diastereomers had significant differences in dearomative [3,3] reactivity: diastereomer **1ii** proceeded with full conversion and 75% isolated yield of **3ii** as a single diastereomer. The stereochemistry of this product was fully characterized by detailed NMR analysis.[35] Under analogous reaction conditions, *iso*-**1ii** was less reactive

and only proceeded to ~5% conversion. Similarly, the 4-NPhth-cyclohexylidenemalononitrile **4r** is prochiral. It was found that the coupling yields two inseparable diastereomers **1jj** and *iso*-**1jj**. Dearomative Cope rearrangement at 75 °C results in 31% conversion of the mixture. A 15% yield of **3jj** was obtained. In the final example in Figure 5, the chiral racemic Sertaline ketone-derived alkylidenemalononitrile **4s** was coupled with the model electrophile **5a** resulting in two inseparable diastereomers **1kk** and *iso*-**1kk**. Both starting materials reacted favorably *via* dearomative Cope rearrangement to their respective products **3kk** and *iso*-**3kk** in high yield and diastereoselectivity, albeit as an inseparable mixture.

To complete our initial studies on the indole-dearomatizing Cope rearrangement, we examined how scaffolds can be made enantioselectively as well as ways in which the Cope products can be derivatized (Figure 6). Regarding enantioselectivity (Figure 6A), we envisaged a Pd-catalyzed kinetic resolution of the racemic electrophile **5a** to the enantioenriched Pd-π-indolyl intermediate.[40,41] In turn, this would react with the

Figure 6. A: *The sequence shows promise for enantioselectivity.* **B:** *The dearomative Cope products 3 are valuable building blocks for preparing functional small molecules 7.*
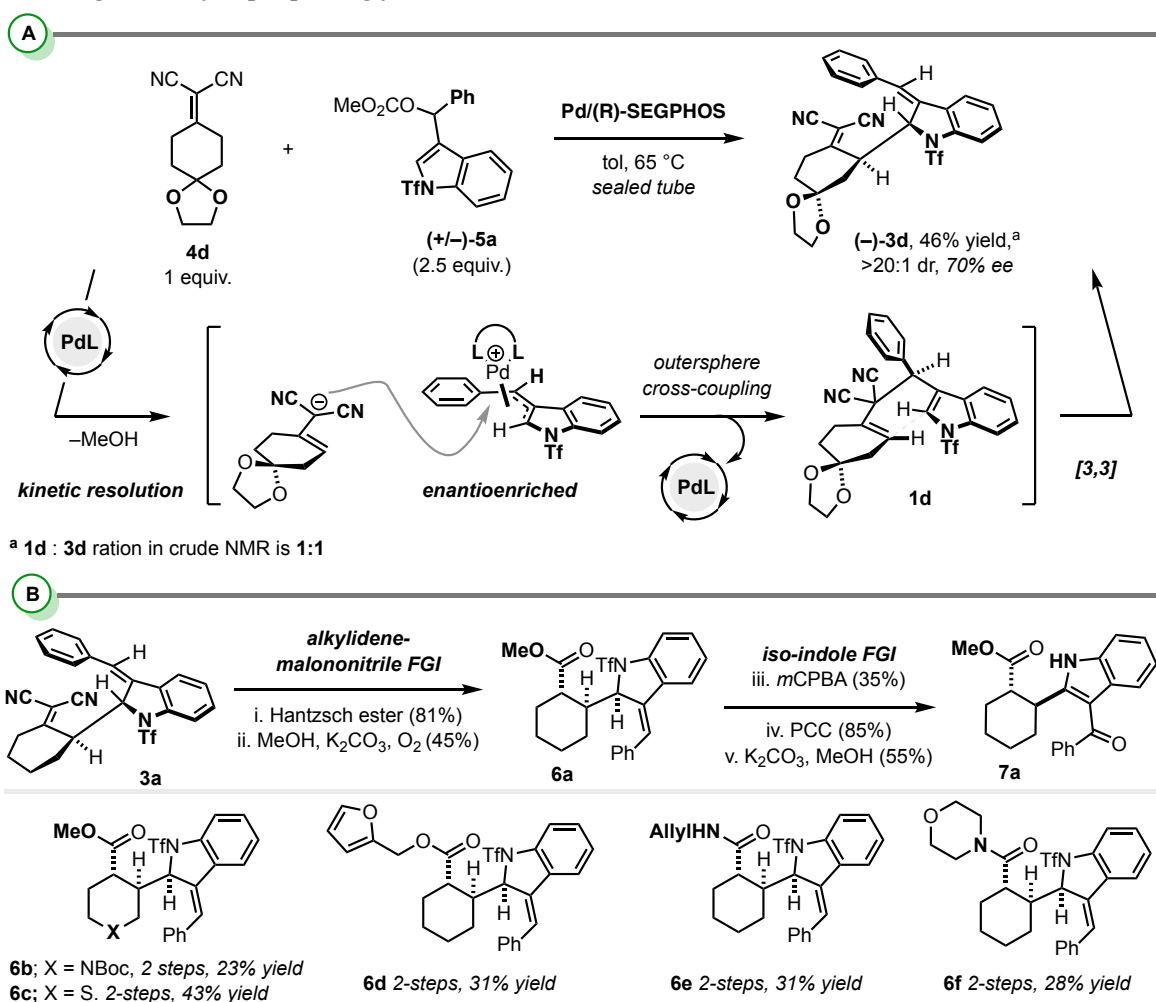
malononitrile-stabilized allyl anion *via* outer-sphere deconjugative benzylation yielding the key scaffold **1d** enantioenriched. Dearomative Cope rearrangement would yield the targeted product **3d** enantioenriched. Indeed, it was found that Pd$_2$dba$_3$/(R)-SEGPHOS provided proof-of-concept enantioselectivity (46% yield of (–)-**3d**, 70% ee) for this sequence. Regarding the functional group interconversion (Figure 6B), it was found that the alkylidenemalononitrile could be reduced efficiently with Hantzsch ester (*step i.*).[42] Next, it was found that various malononitriles could be converted to their respective esters[43] **6a – 6c** or amides[44] in good to modest unoptimized yields using Lear and Hayashi's protocol. The dearomatized indole portion of the scaffold could be rearomatized under oxidative conditions. We examined a two-step procedure involving *m*CPBA oxidation to the carbinol (alkene epoxidation followed by rearomatization) and PCC oxidation to the indole–phenyl ketone. Finally, it was found that the triflate protecting group can also be removed under mildly basic conditions.

CONCLUSIONS

Described herein is a platform for achieving indole-dearomative Cope rearrangement. The key structural features for the kinetic- and thermodynamically favorable dearomative transformation, as determined through computational analysis, are a suite of minor contributing features, including steric congestion of the starting material and product stabilization through resonance conjugation and π-π* aromatic stacking between the newly generated alkylidenemalononitrile and the *trans*-stilbene. Thus, compounding individual minor *substrate-destabilizing* and *product-stabilizing* effects results in thermodynamically favorable dearomatization. The understanding that minor driving forces built into a substrate can amount to a successful transformation that is normally considered kinetically and thermodynamically unfavorable will allow for much continued study, both fundamental and applied. On this line, a key future study will be the design of substrates capable of undergoing dearomative Cope rearrangement *beyond indole*. Herein the scope and limitations of the transformation have been outlined resulting in many successful examples of complex and diverse building blocks. Key to diversity is that the

building blocks are rapidly assembled from alkylidenemalononitriles and indole-phenylmethanol derivatives. These findings suggest that the transformation will be valuable for complex molecule synthesis. On this line, we have provided proof-of-concept findings related to enantioselective synthesis and representative ways that the functional groups on the scaffold can be manipulated. As such, future studies will include further exploration of enantioselectivity and identifying targets to apply this synthetic strategy toward.

ASSOCIATED CONTENT

Supporting Information includes experimental procedures and characterization data (^{1}H NMR, ^{13}C NMR, ^{19}F, HRMS, X-ray, HPLC traces).

ACKNOWLEDGEMENTS

References Cited:

1. Trost, B. M. & Toste, F. D. Asymmetric O- and C-Alkylation of Phenols. *J. Am. Chem. Soc.* **120**, 815–816 (1998).

2. Ito, H., Sato, A. & Taguchi, T. Enantioselective aromatic Claisen rearrangement. *Tetrahedron Lett.* **38**, 4815–4818 (1997).

3. Shrives, H. J., Fernández-Salas, J. A., Hedtke, C., Pulis, A. P. & Procter, D. J. Regioselective synthesis of C3 alkylated and arylated benzothiophenes. *Nat. Commun.* **8**, 14801 (2017).

4. Huang, X. & Maulide, N. Sulfoxide-Mediated α-Arylation of Carbonyl Compounds. *J. Am. Chem. Soc.* **133**, 8510–8513 (2011).

5. Yanagi, T., Otsuka, S., Kasuga, Y., Fujimoto, K., Murakami, K., Nogi, K., Yorimitsu, H., Osuka, A. Metal-Free Approach to Biaryls from Phenols and Aryl Sulfoxides by Temporarily Sulfur-Tethered

Regioselective C–H/C–H Coupling. *J. Am. Chem. Soc.* **138**, 14582–14585 (2016).

6. Alshreimi, A. S., Zhang, G., Reidl, T. W., Peña, R. L. Koto, N.-G., Islam, S. M. Wink, D. J. Anderson, L. L. Synthesis of Spirocyclic 1-Pyrrolines from Nitrones and Arynes through a Dearomative [3,3']-Sigmatropic Rearrangement. *Angew. Chemie Int. Ed.* **59**, 15244–15248 (2020).

7. Fukui, Y., Kobayashi, T., Kawasaki, T., Yamada, F. & Somei, M. A [3,3] sigmatropic and novel ipso [3,3] sigmatropic rearrangement of 1-hydroxyindole chemistry. *Heterocycles* **99**, 465–483 (2019).

8. Huang, S., Kötzner, L., De, C. K. & List, B. Catalytic Asymmetric Dearomatizing Redox Cross Coupling of Ketones with Aryl Hydrazines Giving 1,4-Diketones. *J. Am. Chem. Soc.* **137**, 3446–3449 (2015).

9. Nair, V. N., Kojasoy, V., Laconsay, C. J., Kong, W. Y., Tantillo, D. J., Tambar, U. K. Catalyst-Controlled Regiodivergence in Rearrangements of Indole-Based Onium Ylides. *J. Am. Chem. Soc.* **143**, 9016–9025 (2021).

10. Tayama, E. & Sotome, S. Dearomative [2,3] sigmatropic rearrangement of ammonium ylides followed by 1,4-elimination to form α-(*ortho*-vinylphenyl)amino acid esters. *Org. Biomol. Chem.* **16**, 4833–4839 (2018).

11. Berger, R., Ziller, J. W. & Van Vranken, D. L. Stereoselectivity of the Thia-Sommelet [2,3]-Dearomatization. *J. Am. Chem. Soc.* **120**, 841–842 (1998).

12. Li, G.-Q., Gao, H., Keene, C., Devonas, M., Ess, D. H., Kürti, L. Organocatalytic Aryl–Aryl Bond Formation: An Atroposelective [3,3]-Rearrangement Approach to BINAM Derivatives. *J. Am. Chem. Soc.* **135**, 7414–7417 (2013).

13. Peruzzi, M. T., Lee, S. J. & Gagné, M. R. Gold(I) Catalyzed Dearomative Claisen Rearrangement of Allyl, Allenyl Methyl, and Propargyl Aryl Ethers. *Org. Lett.* **19**, 6256–6259 (2017).

14. Chen, P.-F., Zhou, B., Wu, P., Wang, B. & Ye, L.-W. Brønsted Acid Catalyzed Dearomatization by Intramolecular Hydroalkoxylation/Claisen Rearrangement: Diastereo- and Enantioselective Synthesis of Spirolactams. *Angew. Chemie Int. Ed.* **n/a**, (2021).

15. Saito, A., Kanno, A. & Hanzawa, Y. Synthesis of 2,3-Disubstituted Indoles by a Rhodium-Catalyzed Aromatic Amino-Claisen Rearrangement of *N*-Propargyl Anilines. *Angew. Chemie Int. Ed.* **46**, 3931–3933 (2007).

16. Han, L., Li, S.-J., Zhang, X.-T. & Tian, S.-K. Aromatic Aza-Claisen Rearrangement of Arylpropargylammonium Salts Generated in situ from Arynes and Tertiary Propargylamines. *Chem. – A Eur. J.* **27**, 3091–3097 (2021).

17. Maity, P., Pemberton, R. P., Tantillo, D. J. & Tambar, U. K. Bronsted Acid Catalyzed Enantioselective Indole Aza-Claisen Rearrangement Mediated by an Arene CH-O Interaction. *J. Am. Chem. Soc.* **135**, 16380–16383 (2013).

18. Šiaučiulis, M., Sapmaz, S., Pulis, A. P. & Procter, D. J. Dual vicinal functionalisation of heterocycles via an interrupted Pummerer coupling/[3,3]-sigmatropic rearrangement cascade. *Chem. Sci.* **9**, 754–759 (2018).

19. Eberhart, A. J. & Procter, D. J. Nucleophilic ortho-Propargylation of Aryl Sulfoxides: An Interrupted Pummerer/Allenyl Thio-Claisen Rearrangement Sequence. *Angew. Chemie Int. Ed.* **52**, 4008–4011 (2013).

20. Boyarskikh, V., Nyong, A. & Rainier, J. D. Highly Diastereoselective Sulfonium Ylide Rearrangements to Quaternary Substituted Indolines. *Angew. Chemie Int. Ed.* **47**, 5374–5377 (2008).

21. Burns, J. M., Krenske, E. H. & McGeary, R. P. Claisen rearrangements of benzyl vinyl ethers and heterobenzyl vinyl ethers. *Synthesis (Stuttg).* **50**, 1750–1772 (2018).

22. Biswas, B. & Singleton, D. A. Controlling Selectivity by Controlling the Path of Trajectories. *J. Am. Chem. Soc.* **137**, 14244–14247 (2015).

23. Heravi, M. M., Rohani, S., Zadsirjan, V. & Zahedi, N. Fischer indole synthesis applied to the total synthesis of natural products. *RSC Adv.* **7**, 52852–52887 (2017).

24. Hiersemann, M. & Jaschinski, T. Selected diastereoselective reactions. Diastereoface-differentiating Claisen, Cope, and [2,3]-Wittig rearrangements in contemporary natural product synthesis. in *Compr.*

Chirality vol. 2 625–647 (Elsevier B.V., 2012).

25. Marvell, E. N. & Almond, S. W. The aromatic Cope rearrangement: activation parameters. *Tetrahedron Lett.* 2777–2778 (1979) doi:10.1016/S0040-4039(01)86413-3.

26. Paquette, L. A. Recent applications of anionic oxy-Cope rearrangements. *Tetrahedron* **53**, 13971–14020 (1997).

27. Tomiczek, B. M. & Grenning, A. J. Aromatic Cope rearrangements. *Org. Biomol. Chem.* **19**, 2385–2398 (2021).

28. Gritsch, P. J., Stempel, E. & Gaich, T. Enantioselective Synthesis of Cyclohepta[b]indoles: Gram-Scale Synthesis of (S)-SIRT1-Inhibitor IV. *Org. Lett.* **15**, 5472–5475 (2013).

29. Häfner, M., Sokolenko, Y. M., Gamerdinger, P., Stempel, E. & Gaich, T. Enantioselective Synthesis of Cyclohepta[b]indoles via Pd-Catalyzed Cyclopropane C(sp3)–H Activation as a Key Step. *Org. Lett.* **21**, 7370–7374 (2019).

30. Allegre, K. & Tunge, J. Aryl vinyl cyclopropane Cope rearrangements. *Tetrahedron* **75**, 3319–3329 (2019).

31. Jung, M. E. & Hudspeth, J. P. Anionic oxy-Cope rearrangements with aromatic substrates in bicyclo[2.2.1]heptene systems. Facile synthesis of cis-hydrindanone derivatives, including steroid analogs. *J. Am. Chem. Soc.* **100**, 4309–4311 (1978).

32. Babinski, D. J. *et al.* Synchronized Aromaticity as an Enthalpic Driving Force for the Aromatic Cope Rearrangement. *J. Am. Chem. Soc.* **134**, 16139–16142 (2012).

33. Fereyduni, E., Sanders, J. N., Gonzalez, G., Houk, K. N. & Grenning, A. J. Transient [3,3] Cope rearrangement of 3,3-dicyano-1,5-dienes: computational analysis and 2-step synthesis of arylcycloheptanes. *Chem. Sci.* **9**, 8760–8764 (2018).

34. Fereyduni, E., Lahtigui, O., Sanders, J. N., Tomiczek, B. M., Mannchen, M. D., Yu, R. A., Houk, K. N., Grenning, A. J. Overcoming Kinetic and Thermodynamic Challenges of Classic Cope Rearrangements. *J. Org. Chem.* **86**, 2632–2643 (2021).

35. See the Supporting information for details.

36. Laplaza, R. *et al*. NCIPLOT and the analysis of noncovalent interactions using the reduced density gradient. *WIREs Comput. Mol. Sci.* **11**, e1497 (2021).

37. Contreras-García, J. *et al*. NCIPLOT: A Program for Plotting Noncovalent Interaction Regions. *J. Chem. Theory Comput.* **7**, 625–632 (2011).

38. Krenske, E. H. & Houk, K. N. Aromatic Interactions as Control Elements in Stereoselective Organic Reactions. *Acc. Chem. Res.* **46**, 979–989 (2013).

39. Zha, G.-F., Rakesh, K. P., Manukumar, H. M., Shantharam, C. S. & Long, S. Pharmaceutical significance of azepane based motifs for drug discovery: A critical review. *Eur. J. Med. Chem.* **162**, 465–494 (2019).

40. Mao, B., Ji, Y., Fañanás-Mastral, M., Caroli, G., Meetsma, A., Feringa, B. L. Highly Enantioselective Synthesis of 3-Substituted Furanones by Palladium-Catalyzed Kinetic Resolution of Unsymmetrical Allyl Acetates. *Angew. Chemie Int. Ed.* **51**, 3168–3173 (2012).

41. Li, T.-R., Maliszewski, M. L., Xiao, W.-J. & Tunge, J. A. Stereospecific Decarboxylative Benzylation of Enolates: Development and Mechanistic Insight. *Org. Lett.* **20**, 1730–1734 (2018).

42. Mannchen, M. D., Ghiviriga, I., Abboud, K. A. & Grenning, A. J. 1,2,4-Trifunctionalized Cyclohexane Synthesis via a Diastereoselective Reductive Cope Rearrangement and Functional Group Interconversion Strategy. *Org. Lett.* **23**, 8804–8809 (2021).

43. Hayashi, Y., Li, J., Asano, H. & Sakamoto, D. Sterically Congested Ester Formation from α-Substituted Malononitrile and Alcohol by an Oxidative Method Using Molecular Oxygen. *European J. Org. Chem.* **2019**, 675–677 (2019).

44. Li, J., Lear, M. J. & Hayashi, Y. Sterically Demanding Oxidative Amidation of α-Substituted Malononitriles with Amines Using O_2. *Angew. Chemie Int. Ed.* **55**, 9060–9064 (2016).